THE JOURNAL OF PHYSICAL CHEMISTRY B
A JOURNAL OF THE AMERICAN CHEMICAL SOCIETY

pubs.acs.org/JPCB Article

Solutions and Condensed Phases of PEG_{2000} from All-Atom Molecular Dynamics

Daniel Sponseller and Estela Blaisten-Barojas*

Cite This: https://doi.org/10.1021/acs.jpcb.1c06397 Read Online

ABSTRACT: Extensive all-atom molecular dynamics studies of polyethylene glycol (PEG_{2000}) when solvated and in the polymer bulk condensed phases were performed across a wide temperature range. We proposed two modified all-atom force field and observed the fate of the PEG_{2000} macromolecule when solvated in water, water with 4% ethanol, and ethyl acetate. In aqueous solutions, the macromolecule collapsed into a prolate spheroidal ball-like structure while adopting a rather elongated coiled structure in ethyl acetate. Inspection of the polymer-condensed phases across the 150−340 K temperature range enabled the atomistic view of the solid glass below the glass transition temperature of 230 K < T_g < 250 K and the rubber behavior above T_g. Predicted properties include the enthalpy, density, and cohesive energy temperature behavior, the specific heat, thermal expansivity, thermal compressibility, bulk modulus, and Hildebrand solubility parameter both below and above T_g. Within the polymer matrix, the PEG_{2000} macromolecules were entangled displaying a wide distribution of sizes that persisted when transitioning from the glass to the rubbery phases. Calculated properties agree very well with experiments when available or stand as crucial predictions while awaiting experimental measurement. Understanding the thermodynamics and structure of this useful polymer enables the efficient prediction of its behavior when building novel composite materials for nanomedicine and nanotherapeutics.

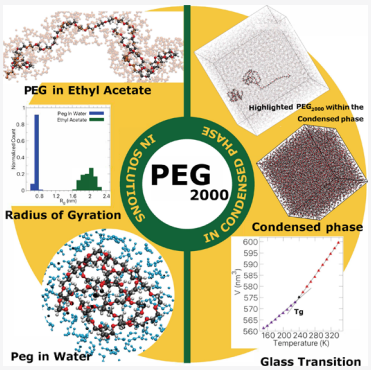

1. INTRODUCTION

Polyethylene glycol (PEG) or poly(ethylene)oxide (PEO or POE) is a polymer commonly used in a range of applications from protein purification and separation processes, liquid−liquid extraction, to drug delivery systems for biomedical applications.[1−3] The latter has sparked interest on PEG's ability to enhance drug encapsulation in polymeric nanoparticles for therapeutic applications.[4−7] Polymers with molecular weight (M_w) below 30,000 u are referred to as PEG, while PEO or POE term polymers with higher M_w.[8] A PEG aqueous two-phase system is extensively used to purify biomaterials in numerous experimental and industrial remediation processes.[9,10] There is increasing interest in phospholipid-PEG copolymers as amphiphilic materials in drug delivery and imaging applications for achieving improved encapsulation efficiency, enhanced nanocarrier stability, and targeted functionalities.[11−13] Experimentally, a high purity PEG_{16} monomethyl ether crystallized unraveling an extended helical secondary structure with 3_{10}-helix strands of different handedness packed in anti-parallel fashion.[14] High-purity PEG_{2000} with a mean M_w of 2000 u is available from various vendors for research applications, currently, being an ingredient in the Pfizer-BioNTech, Moderna, and Janssen COVID-19 vaccines.[15]

Various atomistic simulations have been done on PEG, PEO, and POE. The early simulation of Tasaki[16] found that the solvent influences the structure of PEG in a dramatic manner. Through a molecular dynamics (MD) simulation of POE and PEG, this author demonstrated that the polymer chain collapses into a ball-like structure in the gas phase but displays a helical structure in aqueous solution. Two atomistic studies[17,18] found that POE does not behave as an ideal random coil polymer, observing that in water the polymer radius of gyration (R_g) varies with the concentration; the effect was attributed to a concentration-dependent hydrogen bonding content between POE and water. Another atomistic simulation[19] analyzed PEO chains with up to 36 repeating units modeled with a modified C35 CHARMM in TIP3P water and confirmed that the power law relation between R_g and M_w yielded an exponent of about 0.51; the polymer conformations behaved as ideal coil polymers in a θ solvent[20] instead of acquiring continuous helical domains. Other studies, however, found conflicting conformations of PEG in aqueous solutions depending on the force field (FF) used.[21] In another MD study of PEG in the water solution using the Amber FF, the authors report that the helical regions persist over a few ns for various chain lengths.[22] The OPLS-AA FF was used in an atomistic simulation[23] reporting that in water, the power law

Received: July 17, 2021
Revised: October 22, 2021

relation $R_g \propto n^{0.5}$ was satisfied, with n being the number of monomers. The 0.5 exponent characterizes an ideal random coil polymer chain modeled by random walk paths.[20] A MD-DFT study of low M_w PEG of two to five repeating units[24] reported that intramolecular hydrogen bonding played an important stabilizing role in the short oligomer structures. Meanwhile, along a modeling study fitting polymer lattice models of self-avoiding walks to MD simulations of PEO with up to 33 repeating units in explicit water,[25] it was concluded that the universality class behavior for the short chains was violated; the MD-simulated polymers were more compact with fractal dimension 2 instead of the expected value of 1.73 observed experimentally in PEO with 2 orders of magnitude higher M_w.[26] Recent MD studies of the polymer poly(lactic acid-*co*-glycolic acid) in solutions[27,28] demonstrated that the restrained electrostatic potential atomic charge scheme[29] reproduced mechanical properties of the polymer more accurately to the experimental values than the bond charge correction method applied by default in the generalized Amber FF (GAFF).[30] For PEG, two approaches reached similar observations when implementing the FF with more appropriate atomic charges, the CHARMM C36[31] and the OPLS-AA.[32] MD simulations addressing the behavior of PEGylated compounds, including proteins and peptides, in both implicit and explicit solvents are abundant and covered in a recent review paper.[33]

Efforts in the direction of coarse-grained modeling have been undertaken for studying larger PEG macromolecules. Typically, in these coarse-grained approaches, one monomer unit $-[O-CH_2-CH_2]-$ is represented as a united super atom. A coarse-grained model[34] was developed based on a battery of atomistic simulations of DME and POE short chains.[35] These authors were able to reproduce structural properties but acknowledged that their approach would not be useful for simulating dynamic and thermodynamic properties of POE in solution. Another group[36] fitted their coarse-grained model to atomistic reference simulations and experimental data. They report finding a decreasing R_g as the polymer concentration increases, in agreement with small-angle neutron scattering measurements. The MARTINI coarse-grained model[37] was used to MD simulate the formation of PEG-lipid patches on nanoparticles,[13] pointing out to the substantial physical unknowns in the aggregation processes that preclude the coarse-grained model[38] for the patches' fine structure determination. Hybrid all-atom/coarse-grained modeling has been attempted,[39] showing dependence of PEG chains hydration with polymer length for oligomers with 20 or less repeating units.

In this work, we develop new PEG atomic charges for the all-atom GROMOS 54A7[40] FF and for the GAFF 2020[30] aiming to follow with MD the structural fate of PEG_{2000} solvated in water, water−ethanol, and ethyl acetate. Moreover, with our custom FF, we analyzed the thermodynamic and structural characteristics of the condensed phases of a system of 216 PEG_{2000} macromolecules along the caloric curve spanning a wide temperature range. These results compared very well with the experimental values available in the literature. The paper is organized as follows. In Section 2, we describe the simulation protocol used and construct the molecular model for PEG_{2000}. Section 3.1 has results and discussion of a single PEG_{2000} macromolecule in various solutions and reports on the various properties of the polymer conformations. We then apply our implemented FF to a condensed system of PEG_{2000} macromolecules, along with the reporting of multiple properties of the condensed phases within a 150−340 K temperature range at ambient pressure, as discussed in Section 3.2. Section 4 concludes this paper. The Supporting Information provides plots, tables, and FF parameter files that supplement the material in the sections of this paper.

2. METHODS AND MODELS

A PEG macromolecule of 2000.34 u M_w, $H-(O-CH_2-CH_2)_{45}-OH$, is composed of 45 ethylene oxide repeating units with a total of 318 atoms. We refer to this macromolecule as PEG_{2000}. The atomic charges for the all-atom GROMOS 54A7 FF[40] were determined for 44 backbone repeating units $-(CH_2-O-CH_2)$ with mass m = 44.05176 u and two end residues $-(CH_2-OH)$ with mass m = 31.03322 u. Thereafter, the repeating units and end residues are termed monomers. The initial PEG_{2000} chain structure to be solvated in the three solvents was a helical strand,[14] visualized in Figure S1 of Supporting Information. The helical structure was further optimized using the automated topology builder,[41] and the Mulliken atomic charges were collected. This process determined the FF parameters, including the atomic charges listed in Table 1. Bond interactions were modeled with the Morse potential. Following an equivalent procedure, FF parameters were determined for ethanol, while atomic charges for ethyl acetate were developed previously within our group.[27] All other FF parameters are included in the topology files provided in the SI appendix. The SPC/E and TIP4P models were used for water.

Table 1. Partial Atomic Charges Used in the GROMOS 54A7 Force Field

end residue monomer		backbone monomer	
atom	q_i (e)	atom	q_i (e)
H_O	0.189		
O	−0.313	O	−0.272
C	0.062	C	0.054
H_C	0.031	H	0.041

In order to simulate three solution systems of approximately the same final volume that held comfortably inside one elongated PEG_{2000} macromolecule, three cubic computational boxes with 10 nm edge length were built. Each system was initialized with one solvated macromolecule by adding to the computational boxes a number of solvent molecules consistent with the pure solvent experimental densities reported in Table S2 of Supporting Information. This process led to solution systems with 33,959 water molecules, 31,131:506 water/ethanol molecules, and 6100 EA molecules. Initially, the solvated macromolecule was in its helical structure, while the solvent molecules were all identical but placed randomly within their box. Each system was relaxed by minimizing the full configuration potential energy. The relative PEG_{2000} concentration by mass in these systems was 0.333% in the water and water/ethanol systems and 0.37% in the EA system.

MD simulations were performed using the GROMACS 2019−2020[42−45] software package and both, the all-atom GROMOS 54A7 FF and GAFF, with our custom generated atomic charges. Extensive *NVT* and *NPT* MD simulations were run with the GROMACS implementation of the temperature rescaling and Berendsen pressure couplings,[44] the velocity

https://doi.org/10.1021/acs.jpcb.1c06397
J. Phys. Chem. B XXXX, XXX, XXX−XXX

Verlet integrator, a 1 fs time step, periodic boundary conditions, and a cutoff of 1.5 nm. The Verlet neighbor list scheme with a buffer of 5.0×10^{-5} and the particle mesh Ewald long-range electrostatics with a grid spacing of 0.15 nm and interpolation order of 6 were used. Simulations were first *NPT* equilibrated for 8 ns at 300 K and 101.325 kPa, which ensured fluctuations in the density of less than 0.2%. Solution densities and enthalpies are reported in Table S2 and Figure S2 of Supporting Information. This equilibration was followed by a short *NVT* MD conducted at 300 K for 5 ps such that the system transitioned smoothly to subsequent MD *NVE* simulations calculated in double precision to ensure energy conservation. Specifically, each of the two aqueous systems was *NVE* re-equilibrated for 8 ns with the temperature fluctuating about ±1% around 300 K. Properties were averaged over the last 2 ns. Meanwhile, in the case of the PEG_{2000} in EA, the system was *NVE* monitored for 25 ns. Properties were calculated over the last 2 ns of these runs and the full configurations of the polymer and solvent were saved every 2 ps for further analysis.

Properties of PEG_{2000} in solution reported in Section 3.1 were obtained from the saved configurations. The polymer inherent structure[46] was calculated by minimizing the PEG_{2000} molecule while restraining all the solvent molecules to be fixed and still. Minimizations were done with the steepest descent method and a round-robin approach, where 10% of the atoms were minimized at a time followed by a final minimization of all atoms. The following properties were calculated systematically: the minimized potential energy of PEG_{2000} (U_{min}), the interaction energy with the fixed solvent $U_{int} = U_{total} - (U_{fixedsolvent} + U_{min})$, the radius of gyration $R_g = \sqrt{\frac{1}{M}\sum_{i=1}^{n} m_i(\mathbf{r}_{icm} - \mathbf{r}_{cm})^2}$, D_{ee} the end-to-end distance between the center of mass of the end monomers, and the orientational order parameter[47,48] $Z = \frac{3}{2}\left[\frac{\sum_{i=1}^{n-1}\cos^2\alpha_i}{(n-1)} - \frac{1}{3}\right]$. Here, n is the number of monomers, M and $\mathbf{r}_{cm}$ are the full macromolecule mass and center of mass position, respectively, while m_i and $\mathbf{r}_{icm}$ are the monomer masses and center of mass positions, respectively. The α_i are angles between the vectors joining the centers of mass of two contiguous monomers and the polymer director vector joining the centers of mass of the chain end monomers. The dihedral angle ϕ was calculated between four contiguous monomer centers of mass.

For the condensed phases system of the PEG_{2000} polymer, many macromolecules were placed in a computational box interacting with our developed all-atom GROMOS 54A7 FF parameters. As mentioned later in Section 3, one PEG_{2000} in water collapses into a globular structure. One of these structures was selected and positioned with random orientations at the sites of a $6 \times 6 \times 6$ cubic lattice to build a condensed system with 216 PEG_{2000}, which sums up to 68688 atoms. A simulation workflow we implemented recently was followed.[28,49] First, a steepest decent minimization was performed followed by an *NPT* MD equilibration run of 50 ns at 400 K and 101.325 kPa. Constraints on the hydrogen atoms were applied with the LINCS algorithm (lincs-order = 4). All other simulation parameters were the same as for the single macromolecule in solution. This completed the initial system construction at 400 K for further condensed system simulations. With the purpose of generating initial configurations at reasonable system densities for a selected set of 20 temperatures between 340 and 150 K, the system was *NPT* re-equilibrated for 5 ns at 400 K and a fast cooling scan to 150 K was performed with a linear decrease in temperature over thirteen million time steps. From this simulation scan, 20 initial system configurations with temperatures spaced by 10 K between 150 and 340 K were identified; each of these configurations served to initiate an independent 16 ns *NPT* MD equilibration/production run at the corresponding selected temperature and 101.325 kPa. This collection of simulations yielded 20 independent system samples at each of the 20 selected temperatures with well-equilibrated density at a pressure p = 101.325 kPa. Each of these runs entailed an implementation using 24 cores with 4 GPUs in the accessed supercomputing cluster.

For determining thermodynamic and energetic properties of the condensed phases, the reported property averages and fluctuations were calculated from the last 4 ns of the *NPT* simulations performed for each of the 20 system samples. For the energetic properties, additional 8 ns *NVT* MD runs were performed at the equilibrium density of each of the 20 samples at their assigned temperatures, with the last 4 ns used for calculating the reported energy averages. The resulting data enabled to describe the caloric curve, enthalpy as a function of temperature $H(T)$ at 101.325 kPa. Volume V and density ρ were also recorded as a function of T at that pressure. Two thermodynamic response functions, isobaric heat capacity $C_p = (\partial H/\partial T)_p$ and volumetric thermal expansion coefficient $\alpha_T = V^{-1}(\partial V/\partial T)_p$, were calculated from the caloric curve. Meanwhile, the fluctuations of the enthalpy and system volume were collected along additional NPT MD runs of 6 ns for calculating the $C_p = (\langle H^2\rangle - \langle H\rangle^2)/(k_B T^2)$ and the isothermal compressibility $\kappa_T = (\langle V^2\rangle - \langle V\rangle^2)/(k_B TV)$, with k_B being the Boltzmann constant. The bulk modulus B was obtained from the inverse of κ_T, while the sonic velocity $s = \sqrt{B/\rho}$. From the *NVT* simulations at temperatures between 150 and 340 K, the potential energy U_i of each of the 216 PEG_{2000} molecules were individually recomputed enabling the calculation of the cohesive energy $E_{coh} = \sum_{i=1}^{216} U_i - E_{total}$, which is closely related to solubility properties, including the Hildebrand solubility parameter $\delta_h = \sqrt{E_{coh}/V_m}$, where V_m is the molar volume of the sample.[50,51]

3. RESULTS AND DISCUSSION

3.1. PEG_{2000} Macromolecule in Solution. The importance of the solvent effect on the structure of the PEG_{2000} macromolecule was evidenced by the multiple MD simulations described in this section. In vacuo at 300 K, the initial PEG_{2000} helical chain collapsed into a prolate spheroid-like structure of small R_g, as shown in Figure S2 of Supporting Information. Three properties, R_g, D_{ee}, and Z, change dramatically from 3.34, 11.01, and 0.38 to 0.71, 1.86, and 0.08 nm, respectively. This behavior is consistent with previous results in the gas phase[16] and the chain-folded prolate spheroid structure R_g is in agreement with other free macromolecule simulations.[52] Meanwhile, *NPT* MD simulations at an average temperature of 300 K showed that PEG_{2000} in two aqueous solutions collapsed into a similar prolate spheroid-like structure in about 3−5 ns, maintaining subsequent R_g fluctuating values without major extensions over time. The relaxation toward equilibrium of both, the R_g and D_{ee} values, is depicted in Figure S3 of Supporting Information. The R_g relaxation behavior is comparable to previously reported values of this macromolecule in water while tethered on one end to a protein

https://doi.org/10.1021/acs.jpcb.1c06397
J. Phys. Chem. B XXXX, XXX, XXX−XXX

peptide.[53] However, the macromolecule in EA kept itself quite elongated even after 70 ns. Indeed, the backbone chain maintained random-like bends more typical of an extended random coiled polymer modeled by self-avoiding random walks in a good solvent,[54] where the macromolecule−solvent interaction enhancing the excluded volume favored elongated coiled conformations. In fact, in EA, the solute−solvent dispersive interactions (Lennard Jones) were stronger than the electrostatic interactions, in contrast of what was observed in the two aqueous solutions. Dominance of dispersive over Coulomb interactions has been observed in simulations of PEG-monolaurate in ethanol.[55] As a test, a second simulation of PEG_{2000} in EA was initiated from the prolate spheroid-like structure obtained in vacuo and yet, the polymer opened up and behaved similarly to our primary simulation after a few nanoseconds at 300 K. Figure S3 of Supporting Information illustrates the time relaxation of both, R_g and D_{ee}, evidencing the macromolecule collapse into globular structures in aqueous solutions and the persistence of elongated coiled macromolecular conformations when solvated in EA. Sample instantaneous structures of PEG_{2000} in the three solvents taken from the equilibrated systems are shown in Figure 1.For

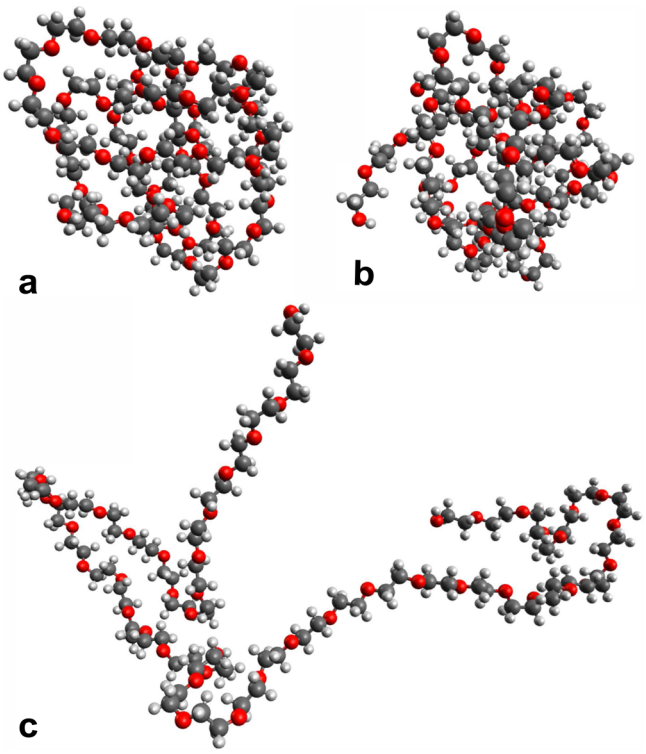

Figure 1. Sample structures of PEG_{2000} in the system equilibrated at 300 K. (a) in water, (b) in mixed water with 4% ethanol, and (c) in ethyl acetate. Color scheme: carbon (gray), oxygen (red), hydrogen (white).

each of the three cases studied, the previously saved 1001 configurations (2 ns) from the MD-production region at 300 K constituted an ensemble of structures that were minimized with restrained solvent molecules to unravel the inherent structure. On the average, five PEG_{2000} properties had the following values in water: U_{min} = 338 ± 30 kJ/mol, U_{int} = −859 ± 50 kJ/mol, R_g = 0.73 ± 0.02 nm, D_{ee} = 1.0 ± 0.3 nm, and Z = 0.1 ± 0.1, where ± stands for one time the standard deviation. Averages of PEG_{2000} in water with 4% ethanol are similar to those in pure water, except that U_{int} is more repulsive and D_{ee} shorter, indicating a tendency of the ethanol molecules of inhibiting free flapping of the macromolecule ends: U_{min} = 359 ± 34 kJ/mol, U_{int} = −883 ± 52 kJ/mol, R_g = 0.74 ± 0.03 nm, D_{ee} = 0.6 ± 0.3 nm, and Z = 0.02 ± 0.09. In EA, the properties related to size showed a significant molecular expansion, the polymeric chain swells increasing the excluded volume. This macromolecule is very flexible evidenced by the D_{ee} behavior over the simulated or averaged times, not excluding that the spanned region of values would be different in longer or alternative simulations. Meanwhile, the energetics evidenced a pronounced stabilization of the polymer structure due to a strongly increased interaction with the solvent. Averages obtained were U_{min} = 721 ± 30 kJ/mol, U_{int} = −1623 ± 62 kJ/mol, R_g = 2 ± 0.1 nm, D_{ee} = 5.8 ± 0.8 nm, and Z = 0.05 ± 0.1. Histograms in Figure 2 illustrate the PEG_{2000} R_g

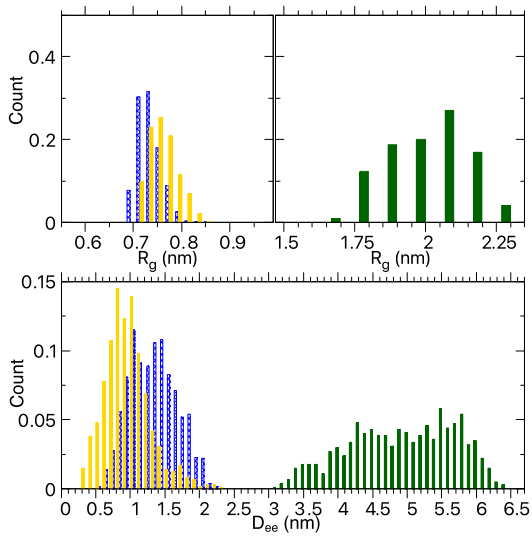

Figure 2. R_g and D_{ee} distributions of PEG_{2000} in solution. Blue is one PEG_{2000} in water, gold is in water with 4% ethanol, and green is in ethyl acetate. Distributions are calculated from the ensemble of the minimized MD configurations corresponding to the inherent structure of the solute in solution.

and D_{ee} distributions of the solute inherent structure. The fluctuations of these properties were indicative of a very flexible polymer in the three solvents studied. The PEG_{2000} properties in solution (potential energy PE, interaction energy with the solvent PE_{int}, R_g, D_{ee}, and Z) minimized along the 2 ns MD production runs at 300 K are provided in Figure S4 of Supporting Information. Additionally, the two aqueous systems were also simulated using the TIP4P for water. Values of the above mentioned polymer properties with this alternative water model were within the standard deviation of results listed above when using the SPC/E model.

Another interesting property is the distribution of dihedral angles (ϕ) between the monomer centers of mass of PEG_{2000}. We computed these ϕ for the set of the minimized configurations. In total, 43,043 dihedral angles were collected, histograms of which are shown in Figure 3. In two aqueous solutions, the macromolecule dihedrals were predominantly below 40° showing a smooth decrease in the frequency as angles increased. This is clear evidence that PEG_{2000} preferred to be folded onto itself giving rise to the globular shape. In ethyl acetate, however, the distribution was almost uniform

https://doi.org/10.1021/acs.jpcb.1c06397
J. Phys. Chem. B XXXX, XXX, XXX−XXX

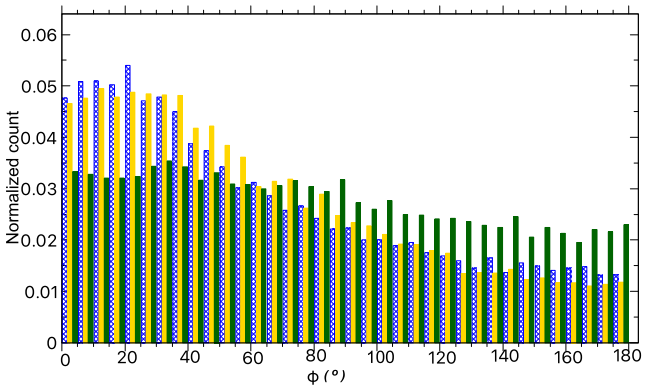

Figure 3. Distribution of PEG_{2000} dihedral angles calculated between the monomers centers of mass when solvated in water (blue), in mixed water/ethanol (gold), and in ethyl acetate (green). Distributions are calculated from the ensemble of the minimized MD configurations corresponding to the inherent structure of the solute in solution.

with a gentle slope favoring slightly the low dihedral angles. Such uniformity was expected from PEG_{2000}-acquired elongated random coiled bends that only fold onto itself for short times due to the flexibility of the macromolecule backbone.

Contemporarily to this paper submission, we completed the modeling of PEG_{2000} and ethanol with GAFF implemented with our custom generated RESP atomic charges.[27,28] Parameters of this alternative FF are reported in the Supporting Information appendix. The most important difference with our previously described FF are the atomic charges. Our custom RESP approach diminishes the over-polarization afforded by the Hartree−Fock with 6-31G* basis set quantum mechanics approach[56] implemented in both, the automated topology builder[41] and the original RESP method.[29] Partial charges matter the most for phenomena in aqueous solutions. Thus for two aqueous solutions, we repeated the MD simulations of the macromolecule now modeled with GAFF-RESP in SPC/E water exactly as described in previous sections and obtained very similar quantitative results. Indeed, the equilibrated densities of the solutions reported in Table S2 of Supporting Information were identical, the PEG_{2000} macromolecule folded in a prolate spheroid-shaped structure with R_g, D_{ee}, and dihedral angle distributions very similar to the histograms of Figures 2 and 3. Summarizing, we are confident that in two aqueous solutions studied with a solute concentration of 0.33% by weight, the all-atom MD simulations at 300 K predict a fast structural relaxation of the PEG_{2000} macromolecule onto a prolate spheroid-globule.

It is known experimentally[26] that PEGs in water display an upper critical solution temperature (UCST) and lower critical solution temperature (LCST) of about 265 and 400 K, respectively. It is also confirmed that aqueous solutions of PEGs of 10^5 u and larger M_w at 303.15 K follow the power law $R_g \propto M_w^{\nu}$ with the exponent $\nu = 0.6$ associated with a good solvent. It is also known that the polymer crystallizes in that size regime. However, for PEGs with M_w in the oligomer regime such as PEG_{2000}, the ν exponent is around 0.5 (its inverse gives the corresponding fractal dimension of 2).[22,39,53] The solid phase of these oligomer-regime macromolecules below 205−250 K is not crystalline.[50] It is additionally believed that the size of the oligomers is too small for allowing the packing of water molecules in the neighborhood of the ether oxygens in a random coil structure. Thus, as a response to the strong electrostatic interaction with the water, the macromolecule tends to minimize the intramolecular excluded volume that consequently gives rise to a compact structure. Coarse-grained modeling to overcome this size deficiency was undertaken[57] through the introduction of temperature-dependent parameters in the interaction model, which conceptually are difficult to justify from the quantum and classical modeling perspectives. In contrast, an organic solvent of low polarity, such as ethyl acetate, displays, under the same modeling approach as in water, much stronger dispersive interactions with the PEG_{2000} that overcome the electrostatic interactions and are able to promote more stretched-out coils in the macromolecule that allow a closer solvent proximity, decreasing the solvent−solute excluded volume at the expense of enhancing it intramolecularly. In fact, without that ability, other than water, polar solvents are prone to producing globular structures of the solvated macromolecular solutes at temperatures between the UCST−LCST.

3.2. Condensed Phases of PEG_{2000}. The condensed system consisted of a cubic box with 216 PEG_{2000} macromolecules. The first goal was generating the caloric curve, enthalpy as a function of temperature. As described in Section 2, independent samples of the system were NPT equilibrated at 20 temperatures between 150 and 340 K yielding the caloric curve depicted in Figure 4a. As expected, the system enthalpy increased as the temperature increased, a characteristic of the condensed matter. Illustrated in Figure 4b is the volume of the condensed system versus temperature revealing an inflection point at around 240 K. To guide the eye, two linear least

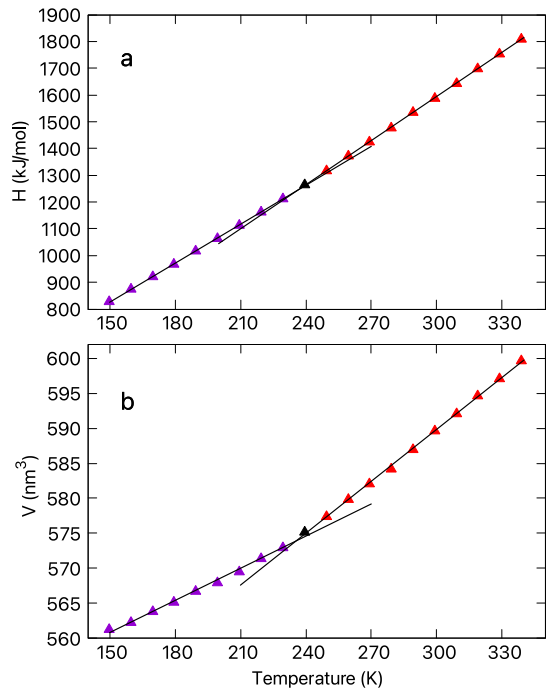

Figure 4. Enthalpy (a) and volume (b) of PEG_{2000}-condensed phases as a function of temperature at p = 101.325 kPa. The inflection point in the volume reveals the glass transition temperature T_g at about 240 K. The linear regression lines are calculated with a custom implementation that minimizes the square error of the fit.

https://doi.org/10.1021/acs.jpcb.1c06397
J. Phys. Chem. B XXXX, XXX, XXX−XXX

squares fits were performed for each property along the 9 lowest and the top 10 temperature points. The clear inflection point of the volume at around 240 K was identified as the glass transition temperature T_g. Below T_g, the system-condensed phase was an amorphous glass. Above T_g and below the melting temperature, the system was in a supercooled region, termed rubber phase in polymer physics. A visual addition to Figure 4b is the density as a function of the temperature plot of Figure S5 of Supporting Information that shows the inflection region around 240 K. The inflection region in polymers is typical of amorphous systems transitioning from the rubber-like state into the glass-like state. The transition temperature region around T_g is, however, a characteristic of the particular polymer with a range 170−500 K across all known synthetic polymers. The more flexible polymers are the lower the T_g region is observed. It was additionally observed that the system density displayed significant increments from the initial configurations as the system approached T_g from higher temperatures. Our T_g determination is in very good agreement with the reported experimental results of 202−251[50] and 250 K for PEG_{4000}[58] despite our in silico cooling rate of 0.47 K/ns, which is orders of magnitude faster that the laboratory experiments. In particular, a calculated average density of 1209 kg/m^3 at 290 ± 1.2 K compares excellently with 1210 kg/m^3 at 293 K reported by commercial suppliers. The caloric curve analysis permitted an immediate determination of the specific heat, C_p, of 2.43 kJ/(kg K) below T_g and 2.75 kJ/(kg K) above T_g, which are somehow larger than the measured 2.16 kJ/(kg K).[50] However, the reported experimental samples are composed of macromolecules of different M_w, thus density and specific heat capacity differences are expected. For example, a C_p in the range 1.95−2.40 kJ/(kg K) was recently reported for a sample of PEG_{1500},[59] while measurements at T = 292 K yielded a value of C_p = 1.81 ± 0.04 kJ/(kg K) for PEG_{2000}[60] with a sharp decrease at lower temperatures. The determination of the glass transition is dependent on the rate of cooling used in the experiments more than on the composing macromolecule mass as reported to be T_g of 213 K for PEG ranging from 3000 to 22,000 u, irrespective of M_w.[61]

In addition, several other properties of the condensed phases are calculated and listed in Table 2. Figure S6 of Supporting Information depicts these properties obtained from fluctuations in the *NPT* simulations within the temperature range of 180−320 K. These fluctuation-based results did not yield smooth curves as a function of increasing temperature, which leads us to adopt estimates based on averaging data points below and above T_g resulting in the values reported in Table 2.

Table 2. Properties of PEG_{2000} Condensed Phases Derived from the Caloric Curve and From Fluctuations in the *NPT* Simulations[a]

	from Figure 4		from fluctuations	
	$<T_g$	$>T_g$	$<T_g$	$>T_g$
C_p (kJ kg^{-1} K^{-1})	2.43	2.75	2.4	2.8
α_T (K^{-1} × 10^{-4})	2.7	4.2	2.7	3.9
κ_T (GPa^{-1})			0.06	0.10
B (GPa)			17.1	11.7

[a]Specific heat capacity C_p, thermal expansion coefficient α_T, thermal compressibility κ_T, and bulk modulus B. Values below T_g ($<T_g$) correspond to 150−230 K. Values above T_g ($>T_g$) correspond to 250−320 K.

The C_p estimates match extremely well the values obtained from the enthalpy in Figure 4a.

The α_T estimates also closely match the reported values of 2−3 × 10^{-4} at temperatures below 300 K and around 6 × 10^{-4} at higher temperatures for PEG_{1000} and PEG_{6000}.[62] This reported α_T value jump, however, occurred around 300 K, when the polymer being above T_g is either a soft amorphous solid or a dense liquid. The authors in that work made no mention to the glass transition temperature. Surprisingly, there exists a limited experimental literature study for the thermal compressibility and bulk modulus of PEG. However, our results for these properties are within the range of known values of polymers with similar characteristics.[50]

The PEG_{2000} cohesive energy E_{coh} in the condensed phases as a function of temperature is shown in Figure 5. As expected,

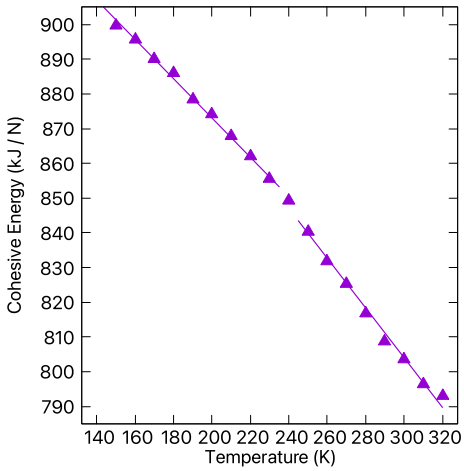

Figure 5. Cohesive energy of the PEG_{2000} condensed phases as a function of temperature for the system with N = 216. At 240 K there is a 3.3852 kJ/N difference between the two fitted lines indicative of a non-linear temperature dependence in the 230−250 K region.

the T_g evidenced in the region 230−250 K from our previous analysis is also apparent from this energetic analysis. From these results and the volume temperature dependence of Figure 4b, we predict the Hildebrand solubility parameter δ_h = 22.1 MPa$^{1/2}$ at 300 K. Our result compares very favorably with other theoretical and experimental reported values between 18 and 25 MPa$^{1/2}$, with most reported values being 21−22 MPa$^{1/2}$.[51,63,64] Figure S7 of Supporting Information illustrates the trend of δ_h as a function of temperature. Considering that solid polymer substances with δ_h similar to that of a solvent will solvate well,[65] we re-assert our findings of Section 3.1 that ethyl acetate, with a solubility parameter of 18.2 MPa$^{1/2}$, solvates adequately the PEG_{2000} condensed sample around 300 K. Indeed, PEG_{2000} solid samples are soluble in EA at ambient conditions. However, we predict that this polymer solubility in EA decreases as the temperature decreases toward the EA freezing point. On the other hand, water has a δ_h of 48 MPa$^{1/2}$, which is above most Hildebrand solubility parameters of solid samples of linear polymers. We have demonstrated in the past[27] that SPC/E or TIP3P water and EA display a clear liquid phase separation, which is expected due to their very different δ_h; these liquids do not mix. Water is a hydrogen bonded, polar, liquid for which other metrics than a comparison between δ_h needs to be considered when evaluating solubility. In the case of PEGs and other thermo-responsive polymers displaying UCST−LCST, determining

https://doi.org/10.1021/acs.jpcb.1c06397
J. Phys. Chem. B XXXX, XXX, XXX−XXX

solubility metrics of the solid samples is complex. More specific experimental evidence is currently needed.

Inspection of the overall size distribution that the macromolecules acquired in the condensed phases, as shown in Figure 6, is indicative of the extensive accommodation that the macromolecules undergo within the computational box, both elongating and entangling. In fact, the distributions of R_g and D_{ee} shown in Figure 6 (top and middle) at 180 and 300 K are consistent with random coiled structures that have elongated significantly from the initial globular structures. Indicative of entanglement between macromolecules was the broad range of D_{ee} with macromolecules having very close end monomers to others with considerable separation between their end monomers. The distribution of the dihedral angles of all the PEG_{2000} macromolecules in the system was quite uniform at all the inspected temperatures, similarly to what is shown in Figure 3 for one macromolecule solvated in ethyl acetate. Meanwhile, Figure 6 (bottom) depicts the distribution of the internal potential energy of the macromolecules at low and ambient temperatures, with both distributions being well fitted by two Gaussian functions peaked at 1469 ± 63, 1382 ± 56 kJ/mol at 180 K, and 1749 ± 63, 1656 ± 58 kJ/mol at 300 K. At low temperatures, the system is a solid with a small group of macromolecules that have lower potential energy due to their smaller R_g. As the system transitioned to a softer condensed phase state, the macromolecules were more extended but due to the entanglement their stretching remained hindered.

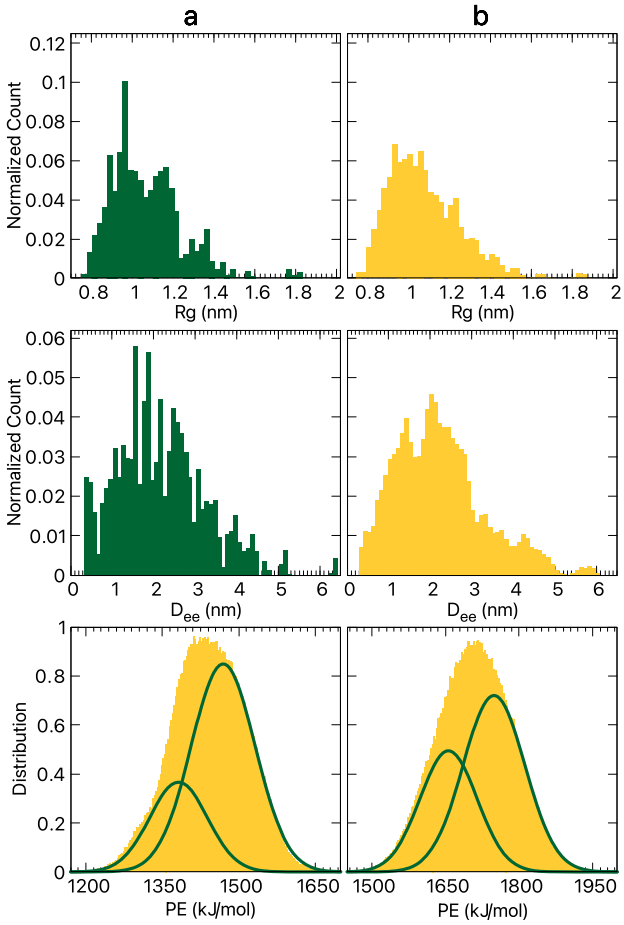

Figure 6. Distributions of PEG_{2000} macromolecule properties in the condensed phase at 180 (a) and 300 K (b). Top: Radius of gyration R_g. Middle: end-to-end distance D_{ee}. Bottom: macromolecules internal potential energy; the two Gaussian functions depicted green are a non-linear least squares fit to the overall energy distribution.

The radial distribution function $g(r)$ between the PEG_{2000} monomers centers of mass of different polymer chains at T = 180 K and T = 300 K is illustrated in Figure 7a and is calculated from eq S1 of Supporting Information. This function clearly indicates below T_g a polymer amorphous glass structure that persists at 300 K indicating that the rubber phase structure is also amorphous. Peculiar of this system structure is that all peaks have approximately the same height instead of favoring the first peak as a larger population of first neighbors and subsequent peaks vanishing in height. This effect reflects how strongly spatially correlated the monomers are which is further exacerbated by the entanglement occurring in the sample. A similar effect was observed recently when analyzing the liquid state.[32] Concurrently, Figure 7b shows the radial distribution for hydrogen−oxygen distances between different macromolecules. The small peak between 0.15 and 0.20 nm is indicative of eventual hydrogen bondings. A close inspection of the configurations revealed that only the hydrogen atoms of the end hydroxyl groups were accommodating within distances and bond alignments compatible with hydrogen bonds between macromolecules. Indeed, at 180 K, about 60% of these hydroxyl H atoms were involved in hydrogen bond formations with the hydroxyl oxygen atoms of other macromolecules and persisted for at least 200 ps. However, at 270 K, only about 46% of the hydroxyl H atoms were involved in hydrogen bondings. Tracking over time 10 of the latter H−O pairs for 200 ps showed that five H separated immediately, one separated after 20 ps, another moved to an adjacent oxygen of a nearby hydroxyl at 20 ps and remained there, while yet another separated after 80 ps, and two pairs persisted within the hydrogen bond distance and angle

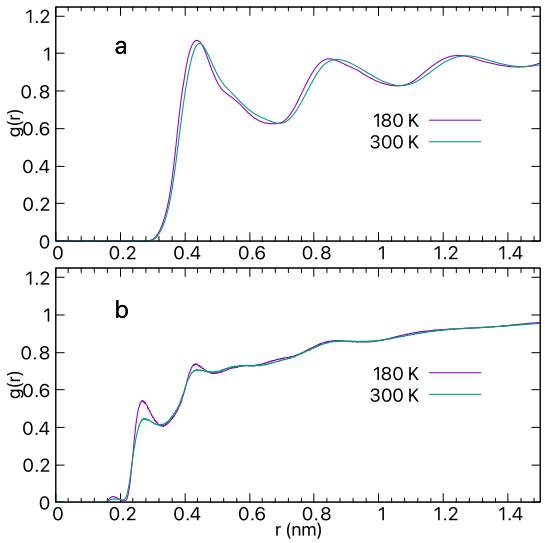

Figure 7. Intermolecular radial distribution functions $g(r)$ at 180 and 300 K. (a) Between the PEG_{2000} monomers centers of mass of different macromolecules and (b) between the oxygens (ether or hydroxyl) and hydrogens (bonded to all heavy atoms) of different macromolecules. Functions were calculated according to eq S1 of Supporting Information that includes the system number density in its normalization.

https://doi.org/10.1021/acs.jpcb.1c06397
J. Phys. Chem. B XXXX, XXX, XXX−XXX

between donor and acceptor bonds during the entire 200 ps time stretch. Meanwhile, at 340 K about 33% of the hydroxyl H atoms met the hydrogen bond criteria although none of them persisted longer than a few ps. It is evident that these inter-macromolecules hydrogen bonds play a role in the glassy phase while becoming transient, coincidental, encounters above T_g, consistent with the system transitioning to a soft amorphous and dense liquid as temperature increases.

4. CONCLUSIONS

In summary, we have modeled a novel protocol for analyzing the PEG_{2000} polymer material by simulating at the nanoscale the polymer behavior when solvated in various solvents and in its condensed phases. This unique inspection enables an effective determination of the macromolecular structure in solution and a robust property identification of the highly entangled glassy polymer matrix. Indeed, PEG_{2000} in water and in water with 4% ethanol collapses into a prolate spheroid structure that continuously rearranges within its prolate spheroid-like volume aided by the strong electrostatic interaction with water that counteracts the intramolecular dispersive forces producing an excluded volume depletion. Contrarily, PEG_{2000} in ethyl acetate resembles an elongated random coiled polymer in a solvent capable of maintaining a swollen coiled structure favored by dominant solute−solvent-dispersive interactions that hinder the aggregation with other macromolecules and enhance the adsorption to other solid polymer surfaces interfacing with ethyl acetate such as polymeric nanoparticles of interest for drug delivery.[13]

The condensed phases of only a few polymers have been inspected from all-atom simulations. This article provides a critical examination of a number of PEG_{2000} properties calculated from atomistic simulations that are comparable to experiments and several others that await experimental determination. Highlighting results that contribute to building PEG_{2000} nanoarchitectures include the enthalpy, density, and cohesive energy as functions of temperature within the 150−340 K range, the thermal expansivity, thermal compressibility, the bulk modulus, cohesive energy, and Hildebrand solubility parameter. Other key calculated factors include the radial distribution function at temperatures below and above the glass transition T_g, indicating that the glassy structure persists even at ambient temperatures. Indeed, insights from the analysis of the individual PEG_{2000} macromolecules within the polymer matrix reveal the presence of a wide range of sizes covering radii of gyration within the 0.8−1.8 nm range, both at temperatures below and above T_g. The calculated features including T_g within 230−250 K, a density of 1209 kg/m^3 at 290 K, and a specific heat C_p of 2.75 kJ/(kg K) at temperatures above T_g are in very good agreement with known experimental values. In a nutshell, this work provides a detailed analysis at the atomic scale of PEG_{2000} in solution and in its condensed phases useful for the challenges and future opportunities in developing composite materials for nanomedicine and nanotherapeutics.

■ ASSOCIATED CONTENT

Supporting Information

The Supporting Information is available free of charge at https://pubs.acs.org/doi/10.1021/acs.jpcb.1c06397.

Add word in green

Content: Rendering of the PEG_{2000} macromolecule; plot of the custom-generated RESP charges of the ether oxygen atoms along the macromolecule, initial macromolecule radius of gyration R_g and end-to-end distance D_{ee}, full solution density and enthalpy during the *NPT* MD time evolution of the three studied solutions containing one PEG_{2000} macromolecule as the solute, temporal relaxation toward equilibrium of the PEG_{2000} radius of gyration and end-to-end distance from its helical structure due to the solvation process, time dependence of the solvated PEG_{2000} internal potential energy PE, interaction energy with the solvent PE_{int}, R_g, D_{ee}, and orientation order parameter Z in the three studied solvents (water, water with 4% ethanol, and ethyl acetate), *NPT* MD values of the 216 macromolecules condensed system as a function of temperature from 150 to 400 K exhibiting the grass transition region around 240 K, temperature dependence of the heat capacity C_p, thermal compressibility κ, and thermal expansion coefficient α calculated from fluctuations along the *NPT* MD at 101.325 kPa in the 180−340 K range, Hildebrand solubility parameter of the PEG_{2000} condensed phases in the 150−320 K range calculated from the *NVT* MD production simulations that followed the *NPT* equilibration, radial distribution function of the equilibrated condensed phases along the *NVT* MD simulation at 180 and 300 K when distributions are normalized with respect to one fixed number density value, and GROMOS 54A7 and GAFF 2020 parameters for the PEG_{2000} macromolecule, ethanol molecule, and ethyl acetate molecule (PDF)

replace highlighted commas by semicolon

delete "and"

■ AUTHOR INFORMATION

Corresponding Author

Estela Blaisten-Barojas − *Center for Simulation and Modeling, and Department of Computational and Data Sciences, George Mason University, Fairfax, Virginia 22030, United States*; orcid.org/0000-0003-3259-1573; Email: blaisten@gmu.edu

Author

Daniel Sponseller − *Center for Simulation and Modeling, and Department of Computational and Data Sciences, George Mason University, Fairfax, Virginia 22030, United States*

Complete contact information is available at: https://pubs.acs.org/10.1021/acs.jpcb.1c06397

Notes

The authors declare no competing financial interest.

■ ACKNOWLEDGMENTS

We acknowledge partial past support from the Thomas F. and Kate Miller Jeffress Memorial Trust. All computations were done in ARGO, the supercomputer cluster of the Office for Research Computing of George Mason University.

■ REFERENCES

(1) D'souza, A. A.; Shegokar, R. Polyethylene Glycol (PEG): a Versatile Polymer for Pharmaceutical Applications. *Expert Opin. Drug Delivery* **2016**, *13*, 1257−1275.

(2) *Poly(ethylene glycol): Chemistry and Biological Applications*; Harris, J. M., Zalipsky, S., Eds.; ACS Symposium Series; American Chemical Society: Washington D.C., 1997; Vol. *680*.

(3) Chen, J.; Spear, S. K.; Huddleston, J. G.; Rogers, R. D. Polyethylene Glycol and Solutions of Polyethylene Glycol as Green Reaction Media. *Green Chem.* **2005**, *7*, 64−82.

(4) Cheng, J.; Teply, B.; Sherifi, I.; Sung, J.; Luther, G.; Gu, F.; Levynissenbaum, E.; Radovicmoreno, A.; Langer, R.; Farokhzad, O. Formulation of functionalized PLGA-PEG nanoparticles for in vivo targeted drug delivery. *Biomaterials* **2007**, *28*, 869−876.

(5) Makadia, H. K.; Siegel, S. J. Poly Lactic-co-Glycolic Acid (PLGA) as Biodegradable Controlled Drug Delivery Carrier. *Polymers* **2011**, *3*, 1377−1397.

(6) Li, Y.-P.; Pei, Y.-Y.; Zhang, X.-Y.; Gu, Z.-H.; Zhou, Z.-H.; Yuan, W.-F.; Zhou, J.-J.; Zhu, J.-H.; Gao, X.-J. PEGylated PLGA Nanoparticles as Protein Carriers: Synthesis, Preparation and Biodistribution in Rats. *J. Controlled Release* **2001**, *71*, 203−211.

(7) Zhang, K.; Tang, X.; Zhang, J.; Lu, W.; Lin, X.; Zhang, Y.; Tian, B.; Yang, H.; He, H. PEG-PLGA copolymers: Their structure and structure-influenced drug delivery applications. *J. Controlled Release* **2014**, *183*, 77−86.

(8) Herzberger, J.; Niederer, K.; Pohlit, H.; Seiwert, J.; Worm, M.; Wurm, F. R.; Frey, H. Polymerization of Ethylene Oxide, Propylene Oxide, and Other Alkylene Oxides: Synthesis, Novel Polymer Architectures, and Bioconjugation. *Chem. Rev.* **2016**, *116*, 2170−2243.

(9) Murugesan, T.; Perumalsamy, M. Liquid−Liquid Equilibria of Poly(ethylene glycol) 2000 + Sodium Citrate + Water at (25, 30, 35, 40, and 45) °C. *J. Chem. Eng. Data* **2005**, *50*, 1392−1395.

(10) Murugesan, T.; Perumalsamy, M. Densities and Viscosities of Polyethylene Glycol 2000 + Salt + Water Systems from (298.15 to 318.15) K. *J. Chem. Eng. Data* **2005**, *50*, 1290−1293.

(11) Hadinoto, K.; Sundaresan, A.; Cheow, W. S. Lipid-polymer hybrid nanoparticles as a new generation therapeutic delivery platform: A review. *Eur. J. Pharm. Biopharm.* **2013**, *85*, 427−443.

(12) Aguilar-Castillo, B. A.; Santos, J. L.; Luo, H.; Aguirre-Chagala, Y. E.; Palacios-Hernández, T.; Herrera-Alonso, M. Nanoparticle Stability in Biologically Relevant Media: Influence of Polymer Architecture. *Soft Matter* **2015**, *11*, 7296−7307.

(13) Salvador-Morales, C.; Brahmbhatt, B.; Márquez-Miranda, V.; Araya-Duran, I.; Canan, J.; Gonzalez-Nilo, F.; Vilos, C.; Cebral, J.; Mut, F.; Lohner, R.; et al. Mechanistic Studies on the Self-Assembly of PLGA Patchy Particles and Their Potential Applications in Biomedical Imaging. *Langmuir* **2016**, *32*, 7929−7942.

(14) French, A. C.; Thompson, A. L.; Davis, B. G. High-purity Discrete PEG-oligomer Crystals Allow Structural Insight. *Angew. Chem., Int. Ed.* **2009**, *48*, 1248−1252.

(15) PEG 2000. https://moleculardepot.com/product/polyethylene-glycol-2000-peg-2000/. (Accessed Dec 09, 2021).

(16) Tasaki, K. Poly(oxyethylene)−Water Interactions: A Molecular Dynamics Study. *J. Am. Chem. Soc.* **1996**, *118*, 8459−8469.

(17) Smith, G. D.; Bedrov, D.; Borodin, O. Conformations and Chain Dimensions of Poly(ethylene oxide) in Aqueous Solution: a Molecular Dynamics Simulation Study. *J. Am. Chem. Soc.* **2000**, *122*, 9548−9549.

(18) Smith, G. D.; Bedrov, D.; Borodin, O. Molecular Dynamics Simulation Study of Hydrogen Bonding in Aqueous Poly(ethylene oxide) Solutions. *Phys. Rev. Lett.* **2000**, *85*, 5583.

(19) Lee, H.; Venable, R. M.; MacKerell, A. D., Jr.; Pastor, R. W. Molecular Dynamics Studies of Polyethylene Oxide and Polyethylene Glycol: Hydrodynamic Radius and Shape Anisotropy. *Biophys. J.* **2008**, *95*, 1590−1599.

(20) Teraoka, I. *Polymer Solutions: An Introduction of Physical Properties*; John Wiley & Sons, Inc., New York, USA, 2002.

(21) Winger, M.; de Vries, A. H.; van Gunsteren, W. F. Force-field dependence of the conformational properties of α,ω-dimethoxypolyethylene glycol. *Mol. Phys.* **2009**, *107*, 1313−1321.

(22) Oelmeier, S. A.; Dismer, F.; Hubbuch, J. Molecular Dynamics Simulations on Aqueous Two-phase Systems-Single PEG-molecules in Solution. *BMC Biophys.* **2012**, *5*, 14.

(23) Mondal, J.; Choi, E.; Yethiraj, A. Atomistic Simulations of Poly(ethylene oxide) in Water and an Ionic Liquid at Room Temperature. *Macromolecules* **2013**, *47*, 438−446.

(24) Kozlowska, M.; Goclon, J.; Rodziewicz, P. Intramolecular Hydrogen Bonds in Low-Molecular-Weight Polyethylene Glycol. *ChemPhysChem* **2016**, *17*, 1143−1153.

(25) Dietschreit, J. C. B.; Diestler, D. J.; Knapp, E. W. Chemically Realistic Tetrahedral Lattice Models for Polymer Chains: Application to Polyethylene Oxide. *J. Chem. Theory Comput.* **2016**, *12*, 2388−2400.

(26) Devanand, K.; Selser, J. C. Asymptotic behavior and long-range interactions in aqueous solutions of poly(ethylene oxide). *Macromolecules* **1991**, *24*, 5943−5947.

(27) Andrews, J.; Blaisten-Barojas, E. Exploring with Molecular Dynamics the Structural Fate of PLGA Oligomers in Various Solvents. *J. Phys. Chem. B* **2019**, *123*, 10233−10244.

(28) Andrews, J.; Handler, R. A.; Blaisten-Barojas, E. Structure, Energetics and Thermodynamics of PLGA Condensed Phases from Molecular Dynamics. *Polymer* **2020**, *206*, 122903.

(29) Bayly, C. I.; Cieplak, P.; Cornell, W.; Kollman, P. A. A Well-behaved Electrostatic Potential Based Method Using Charge Restraints for Deriving Atomic Charges: the RESP Model. *J. Phys. Chem.* **1993**, *97*, 10269−10280.

(30) Wang, J.; Wolf, R. M.; Caldwell, J. W.; Kollman, P. A.; Case, D. A. Development and Testing of a General Amber Force Field. *J. Comput. Chem.* **2004**, *25*, 1157−1174.

(31) Leonard, A. N.; Pastor, R. W.; Klauda, J. B. Parameterization of the CHARMM All-Atom Force Field for Ether Lipids and Model Linear Ethers. *J. Phys. Chem. B* **2018**, *122*, 6744−6754.

(32) Fang, C.-E.; Tsai, Y.-C.; Scheurer, C.; Chiu, C.-C. Revised Atomic Charges for OPLS Force Field Model of Poly(ethylene oxide): Benchmarks and Applications in Polymer Electrolyte. *Polymers* **2021**, *13*, 1131.

(33) Lee, H. Molecular Simulations of PEGylated Biomolecules, Liposomes, and Nanoparticles for Drug Delivery Applications. *Pharmaceutics* **2020**, *12*, 533.

(34) Fischer, J.; Paschek, D.; Geiger, A.; Sadowski, G. Modeling of Aqueous Poly(oxyethylene) Solutions. 2. Mesoscale Simulations. *J. Phys. Chem. B* **2008**, *112*, 13561−13571.

(35) Fischer, J.; Paschek, D.; Geiger, A.; Sadowski, G. Modeling of Aqueous Poly(oxyethylene) Solutions: 1. Atomistic Simulations. *J. Phys. Chem. B* **2008**, *112*, 2388−2398.

(36) Prasitnok, K.; Wilson, M. R. A Coarse-grained Model for Polyethylene Glycol in Bulk Water and at a Water/air Interface. *Phys. Chem. Chem. Phys.* **2013**, *15*, 17093−17104.

(37) Grunewald, F.; Rossi, G.; de Vries, A. H.; Marrink, S. J.; Monticelli, L. Transferable MARTINI Model of Poly(ethylene Oxide). *J. Phys. Chem. B* **2018**, *122*, 7436−7449.

(38) Ramezanghorbani, F.; Lin, P.; Colina, C. M. Optimizing Protein-Polymer Interactions in a Poly(ethylene glycol) Coarse-Grained Model. *J. Phys. Chem. B* **2018**, *122*, 7997−8005.

(39) Stanzione, F.; Jayaraman, A. Hybrid Atomistic and Coarse-Grained Molecular Dynamics Simulations of Polyethylene Glycol (PEG) in Explicit Water. *J. Phys. Chem. B* **2016**, *120*, 4160−4173.

(40) Schmid, N.; Eichenberger, A. P.; Choutko, A.; Riniker, S.; Winger, M.; Mark, A. E.; van Gunsteren, W. F. Definition and Testing of the GROMOS Force-Field Versions 54A7 and 54B7. *Eur. Biophys. J.* **2011**, *40*, 843.

(41) Malde, A. K.; Zuo, L.; Breeze, M.; Stroet, M.; Poger, D.; Nair, P. C.; Oostenbrink, C.; Mark, A. E. An Automated Force Field Topology Builder (ATB) and Repository: Version 1.0. *J. Chem. Theory Comput.* **2011**, *7*, 4026−4037.

(42) Berendsen, H. J. C.; van der Spoel, D.; van Drunen, R. GROMACS: A message-passing parallel molecular dynamics implementation. *Comput. Phys. Commun.* **1995**, *91*, 43−56.

(43) Lindahl, E.; Hess, B.; van der Spoel, D. GROMACS 3.0: a package for molecular simulation and trajectory analysis. *J. Mol. Model.* **2001**, *7*, 306−317.

(44) Van Der Spoel, D.; Lindahl, E.; Hess, B.; Groenhof, G.; Mark, A. E.; Berendsen, H. J. C. GROMACS: Fast, Flexible, and Free. *J. Comput. Chem.* **2005**, *26*, 1701−1718.

https://doi.org/10.1021/acs.jpcb.1c06397
J. Phys. Chem. B XXXX, XXX, XXX−XXX

(45) Hess, B.; Kutzner, C.; van der Spoel, D.; Lindahl, E. GROMACS 4: Algorithms for Highly Efficient, Load-balanced, and Scalable Molecular Simulation. *J. Chem. Theory Comput.* **2008**, *4*, 435−447.
(46) Stillinger, F. H.; Weber, T. A. Inherent Structure in Water. *J. Phys. Chem.* **1983**, *87*, 2833−2840.
(47) Usatenko, Z.; Sommer, J.-U. Calculation of the Segmental Order Parameter for a Polymer Chain in Good Solvent. *Macromol. Theory Simul.* **2008**, *17*, 39−44.
(48) Dai, Y.; Blaisten-Barojas, E. Monte Carlo study of Oligopyrroles in Condensed Phases. *J. Chem. Phys.* **2010**, *133*, 034905.
(49) Andrews, J.; Blaisten-Barojas, E. Workflow for Investigating Thermodynamic, Structural and Energy Properties of Condensed Polymer Systems. In *Advances in Parallel & Distributed Processing, and Applications*; Arabnia, H. R., Deligiannidis, L., Grimaila, M., Hodson, D., Joe, K., Sekijima, M., Tinetti, F., Eds.; CSCE'20 Proceedings: MSV'20, Int'l Conference on Modeling, Simulation and Visualization Methods, June 2020, Las Vegas, NV, USA; Springer Nature, 2021; pp 1033−1039.
(50) CROW, Polymer Properties Database. https://www.polymerdatabase.com/polymers/polyethyleneglycol.html. (Accessed Sept 27, 2021).
(51) Wohlfarth, C. Chapter 13: Solubility Parameters of Selected Polymers. In *CRC Handbook of Chemistry and Physics*, 97th ed.; Hayne, W., Ed.; CRC Press: Boca Raton, FL, USA, 2016; pp 70−71.
(52) Munasinghe, A.; Mathavan, A.; Mathavan, A.; Lin, P.; Colina, C. M. Molecular Insight into the Protein-Polymer Interactions in N-Terminal PEGylated Bovine Serum Albumin. *J. Phys. Chem. B* **2019**, *123*, 5196−5205.
(53) Woo, S. Y.; Lee, H. Molecular Dynamics Studies of PEGylated α-Helical Coiled Coils and Their Self-Assembled Micelles. *Langmuir* **2014**, *30*, 8848−8855.
(54) Sun, S. F. *Physical Chemistry of Macromolecules*; John Wiley & Sons Inc.: New Jersey, USA, 2004.
(55) Khoiroh, I.; Lee, S. Y.; Pirdashti, M.; Lee, M.-J. Insight into Structural Properties of Polyethylene Glycol Monolaurate in Water and Alcohols from Molecular Dynamics Studies. *RSC Adv.* **2020**, *10*, 21760.
(56) Schauperl, M.; Nerenberg, P. S.; Jang, H.; Wang, L.-P.; Bayly, C. I.; Mobley, D. L.; Gilson, M. K. Non-bonded Force Field Model with Advanced Restrained Electrostatic Potential Charges (RESP2). *Commun. Chem.* **2020**, *3*, 44.
(57) Chudoba, R.; Heyda, J.; Dzubiella, J. Temperature-Dependent Implicit-Solvent Model of Polyethylene Glycol in Aqueous Solution. *J. Chem. Theory Comput.* **2017**, *13*, 6317−6327.
(58) PerkinElmer. Application Note: Thermal Analysis. https://resources.perkinelmer.com/lab-solutions/resources/docs/APP_TgandMeltofPolyethylene.pdf. (Accessed Sept 27, 2021).
(59) Egelle, E.; Hamad, F.; Gooneratne, S.; Russell, P. CFD Simulation of Melting Process of Polyethylene Glycol 1500 (PEG1500) in Different Geometry Enclosures. *ISER—373rd International Conference on Heat Transfer and Fluid Flow, August 18−19, 2018*, London, UK, 2018.
(60) Kou, Y.; Wang, S.; Luo, J.; Sun, K.; Zhang, J.; Tan, Z.; Shi, Q. Thermal Analysis and Heat Capacity Study of Polyethylene Glycol (PEG) Phase Change Materials for Thermal Energy Storage Applications. *J. Chem. Thermodyn.* **2019**, *128*, 259−274.
(61) Törmälä, P. Determination of Glass Transition Temperature of Poly(ethylene glycol) by Spin Probe Technique. *Eur. Polym. J.* **1974**, *10*, 519−521.
(62) Tsujita, Y.; Nose, T.; Hata, T. Thermodynamic Properties of Poly(ethylene glycol) and Poly(tetrahydrofuran). I. P-V-T Relations and Internal Pressure. *Polym. J.* **1973**, *5*, 201−207.
(63) Kalam, M. A.; Alshamsan, A.; Alkholief, M.; Alsarra, I. A.; Ali, R.; Haq, N.; Anwer, M. K.; Shakeel, F. Solubility Measurement and Various Solubility Parameters of Glipizide in Different Neat Solvents. *ACS Omega* **2020**, *5*, 1708−1716.
(64) Özdemir, C.; Güner, A. Solubility Profiles of Poly(ethylene glycol)/Solvent Systems, I: Qualitative Comparison of Solubility Parameter Approaches. *Eur. Polym. J.* **2007**, *43*, 3068−3093.
(65) Dimian, A. C.; Bildea, C. S.; Kiss, A. A. Chemical Product Design. In *Integrated Design and Simulation of Chemical Processes*; Dimian, A. C., Bildea, C. S., Kiss, A. A., Eds.; Computer Aided Chemical Engineering; Elsevier, Amsterdam, Netherlands, 2014; Vol. *35*, pp 489−523.

https://doi.org/10.1021/acs.jpcb.1c06397
J. Phys. Chem. B XXXX, XXX, XXX−XXX